JOURNAL OF SOLID STATE CHEMISTRY **140,** 134–139 (1998)
ARTICLE NO. SC987912

Synthesis and Crystal Structure of $Sr_{10}[Sb_7O_{13}(OH)]_2[SbSe_3]_2Se \cdot 2H_2O$

Xiqu Wang and Allan J. Jacobson[1]

Department of Chemistry, University of Houston, Houston, Texas 77204

Received March 2, 1998; in revised form May 20, 1998; accepted May 29, 1998

A new strontium oxoselenoantimonate(III), $Sr_{10}[Sb_7O_{13}(OH)]_2[SbSe_3]_2 \cdot 2H_2O$, has been hydrothermally synthesized and characterized by single crystal structure determination. It crystallizes in the monoclinic system, space group $P2_1/n$, with $a = 11.4013(6)$ Å, $b = 18.417(1)$ Å, $c = 13.0568(7)$ Å, $\beta = 108.51(1)°$, $V = 2599.9(2)$ Å^3, measured at 223 K. In the structure $[SbO_3]$ pyramids share oxygen atoms to form $[Sb_7O_{13}(OH)]$ single branched six-rings that are interconnected by Sr–O bonds into layers with composition $[Sr_5Sb_7O_{13}(OH)]$. The interlayer spaces are occupied by $[SbSe_3]$ pyramids and isolated Se^{2-} anions. Both the $[Sb_7O_{13}(OH)]$ single branched six-rings and the $[SbSe_3]$ pyramids can be considered as building blocks of the known structure $K_6[Sb_{12}O_{18}][SbSe_3]_2 \cdot 6H_2O$. © 1998 Academic Press

INTRODUCTION

Very few oxoselenoantimonates with trivalent antimony are known. However, a few alkali oxoselenoantimonates are reported that are isostructural with the rare mineral cetineite (1). A noteworthy example is $K_6[Sb_{12}O_{18}][SbSe_3]_2 \cdot 6H_2O$, the structure of which was recently reported. This compound shows photosemiconducting properties (2, 3). The structure contains remarkable one-dimensional $[Sb_{12}O_{18}]$ tubes with aperture ca. 7 Å (4). The water molecules contained within the tubes can be reversibly removed at room temperature. The tube walls are built up from $[SbO_3]$ pyramids and the space between the tubes is occupied by isolated $[SbSe_3]$ pyramids. The alkali cations within the tubes can be replaced by divalent cations with simultaneous replace of H_2O by OH^- in order to maintain charge balance. Despite intensive synthetic investigations of this group of compounds (5), the reaction mechanisms involved in the formation of these rather complicated systems remain unknown.

During the synthesis of the cetineite type phase $Sr_6[Sb_{12}O_{18}][SbSe_3]_2(OH)_6$ (5) a novel strontium oxoselenoantimonate, $Sr_{10}[Sb_7O_{13}(OH)]_2[SbSe_3]_2Se \cdot 2H_2O$ (**1**), was obtained. In the crystal structure of **1**, determined from single crystal X-ray diffraction data, seven $[SbO_3]$ pyramids form a unique $[Sb_7O_{13}(OH)]$ single branched six-ring that can be considered as a building block of the infinite $[Sb_{12}O_{18}]$ tubes found in the cetineite type structure. The isolated $[SbSe_3]$ pyramids in **1** are similar to those in the cetineite phases.

EXPERIMENTAL

In a typical synthesis, elemental Sb (0.37 g, 3.0 mmol) and Se (0.30 g, 3.8 mmol) and $LiOH \cdot H_2O$ (0.60 g, 14.2 mmol) were mixed with 2 ml water. $Sr(OH)_2 \cdot 8H_2O$ (0.57 g, 2.2 mmol) was subsequently added to the mixture. Finally the mixture was sealed in air in a Teflon-lined autoclave with 23 ml inner volume and heated at 220°C for four days. The product was washed with water, vacuum filtered, and dried in air. Brown prismatic crystals of the title compound crystallized together with a minor amount of $Sr_6[Sb_{12}O_{18}][SbSe_3]_2(OH)_6$ in the form of tiny dark red crystals.

The composition of the title compound was determined using JEOL 8600 electron microcope operating at 15 KeV with a 10-μm beam diameter and a beam current of 30 nA. Measurements on five crystals gave the average atomic ratios Sr : Sb : Se : O = 5.00 : 8.27 : 3.45 : 15.66, consistent with the formula ratios Sr : Sb : Se : O = 5 : 8 : 3.5 : 15 derived from the structure refinement.

For single crystal X-ray data collection, a fragment with approximate dimensions 0.50 × 0.24 × 0.20 mm was cut off from a large crystal and mounted on a glass fiber using silicon sealant. Intensities were measured on a SMART platform diffractometer equipped with a 1 K CCD area detector using graphite-monochromatized Mo$K\alpha$ radiation at −50°C. A hemisphere of data (1271 frames at detector distance 5 cm) was collected using a narrow-frame method with scan widths of 0.30° in ω and an exposure time of 30 s/frame. The first 50 frames were remeasured at the end of the data collection to monitor instrument and crystal stability, and the maximum correction applied on the intensities was <1%. The data were integrated using the Siemens SAINT program (6), with the intensities corrected for Lorentz factor, polarization, air absorption, and absorption due to variation in the path length through the detector

---

[1] To whom correspondence should be addressed.

0022-4596/98 $25.00

TABLE 1
Crystal Data and Structure Refinement for $Sr_{10}[Sb_7O_{13}(OH)]_2[SbSe_3]_2Se\cdot 2H_2O$

Temperature	223 K
Crystal system	monoclinic
Space group	$P2_1/n$ (No. 14)
Unit cell dimensions	$a = 11.4013(6)$ Å, $b = 18.417(1)$ Å, $c = 13.0568(7)$ Å $\beta = 108.51(1)°$ $V = 2599.9(2)$ Å^3, $Z = 2$
Crystal size	$0.50 \times 0.24 \times 0.20$ mm
Density (calculated)	4.935 g/cm^3
Radiation/wavelength	Mo$K\alpha$/0.71073 Å
Absorption coefficient	23.284 mm^{-1}
Absorption correction	SADABS and DIFABS programs
2θ range for data collection	3.9–56.8°
Limiting indices	$-15 \le h \le 14$, $0 \le k \le 24$, $0 \le l \le 17$
Reflections collected	15,258
Independent reflections	5941 [R(int) = 0.0411]
Refinement method	Full-matrix least-squares on F^2
Data/restraints/parameters	5941/4/297
Goodness-of-fit on F^2	1.067
Final R indices for $I > 2\sigma(I)$	$R1 = 0.0261$, w$R2 = 0.0591$
Final R indices for all data	$R1 = 0.0311$, w$R2 = 0.0609$
Extinction coefficient	0.00003(2)
Largest diff. peak and hole	1.173 and -1.039 eA^{-3}

$R1 = \sum | |F_0| - |F_c| |/\sum|F_0|$, $wR2 = [\sum(w(F_0^2 - F_c^2)^2)/\sum(wF_0^2)^2]^{1/2}$, $w = 1/[\sigma(F_0^2)]^2$

TABLE 2
Atomic Coordinates ($\times 10^4$) and Equivalent Isotropic Displacement Parameters (Å$^2 \times 10^3$) for $Sr_{10}[Sb_7O_{13}(OH)]_2[SbSe_3]_2Se\cdot 2H_2O$, Where U_{eq} Is Defined as One Third of the Trace of the Orthogonalized U_{ij} Tensor

Atoms	x	y	z	U_{eq}
Sb1	− 2330(1)	892(1)	5162(1)	8(1)
Sb2	− 96(1)	974(1)	7805(1)	6(1)
Sb3	3206(1)	873(1)	8230(1)	7(1)
Sb4	− 5717(1)	931(1)	5698(1)	6(1)
Sb5	8054(1)	− 1100(1)	6928(1)	6(1)
Sb6	8691(1)	886(1)	2848(1)	7(1)
Sb7	6163(1)	1561(1)	717(1)	8(1)
Sb8	6079(1)	− 123(1)	8547(1)	10(1)
Sr1	3417(1)	2347(1)	1569(1)	7(1)
Sr2	5954(1)	3431(1)	472(1)	8(1)
Sr3	5144(1)	2257(1)	7754(1)	7(1)
Sr4	6788(1)	2435(1)	3314(1)	7(1)
Sr5	8523(1)	2246(1)	9465(1)	8(1)
Se1	7946(1)	− 858(1)	9688(1)	14(1)
Se2	6997(1)	883(1)	7699(1)	13(1)
Se3	5246(1)	957(1)	6904(1)	12(1)
Se4	0	0	5000	28(1)
O1	− 1764(4)	1369(2)	4035(3)	10(1)
O2	− 932(3)	1323(2)	6298(3)	8(1)
O3	1487(3)	1237(2)	7510(3)	7(1)
O4	− 6468(4)	1155(1)	6844(3)	13(1)
O5	− 7342(3)	1262(2)	4648(3)	9(1)
O6	9737(3)	− 1413(2)	6740(3)	8(1)
O7	7837(3)	− 2100(2)	7247(3)	8(1)
O8	− 5098(3)	1923(2)	5772(3)	7(1)
O9	3782(4)	1801(2)	8823(3)	11(1)
O10	− 226(3)	1942(2)	8305(3)	7(1)
O11	7832(4)	1726(2)	1930(3)	11(1)
O12	5447(3)	2299(2)	1366(3)	8(1)
O13	6534(3)	2222(2)	9731(3)	9(1)
OH	− 3144(3)	1884(2)	5146(3)	7(1)
OW	10762(5)	972(3)	9522(4)	25(1)
H1	3813(90)	2007(70)	5445(94)	114(29)
H2	11297(92)	669(61)	9926(99)	114(29)
H3	9978(74)	921(64)	9522(114)	114(29)

faceplate. Final cell constants were refined using 6762 reflections having $I > 10\sigma(I)$. An adsorption correction was first made using the program SADABS (7) based on equivalent reflections. After solving the structure, a further absorption correction was applied using the program DIFABS (8).

The structure was solved by direct methods and refined using SHELXTL (9). All nonhydrogen positions were derived by direct methods and refined anisotropically in the final refinements. The hydrogen atoms were located from difference maps and refined isotropically with atom distance constraints. Crystallographic and refinement details are summarized in Table 1. Atom positions are given in Table 2 and selected bond lengths and bond angles in Table 3.

STRUCTURE DESCRIPTION AND DISCUSSION

The local coordination environments of the antimony atoms are shown in Fig. 1. The Sb(1–7) atoms are each coordinated to three oxygen atoms to form trigonal pyramids with Sb–O bond length in the range 1.90–2.09 Å and O–Sb–O angles between 81.4° and 94.3°. The coordination environments of Sb(1–6) are further complemented by one or two Se atoms with weak Sb–Se interactions (3.18–3.37 Å). The Sb(8) atom is coordinated by three Se atoms to form an $[SbSe_3]$ pyramid with Sb–Se bond lengths 2.55–2.56 Å and Se–Sb–Se angles between 99.6° and 104.9°. The Sr atoms are each coordinated both by Se atoms with Sr–Se bond lengths 3.30–3.48 Å and by O atoms including water oxygen with Sr–O bond lengths 2.40–2.96 Å. The coordination number of each of the five inequivalent Sr atoms is 7 with such bond length limits. The Sr coordination environments are shown in Fig. 2.

The $[Sb(1)O_2(OH)]$ and $[Sb(2–6)O_3]$ pyramids share oxygen atoms at their corners to form a $[Sb_6O_{11}(OH)]$ six-ring that is attached to the $[Sb(7)O_3]$ pyramid as an single branch (Fig. 1). These $[Sb_7O_{13}(OH)]$ single branched rings are packed parallel to (010) with the $[Sb(7)O_3]$ branches aligned along the [101] direction. An infinite row of these rings are formed through translation symmetry along [101]. Each two such rows are related by a glide plane *n* with Sr(2–4) atoms located between them and are interconnected by the Sr–O bonds into a [101] band. Within the band the Sb(7) atoms (ring branches) of one chain lie approximately over the centers of the rings of another chain. Neighboring bands are interconnected into $[Sr_5Sb_7O_{13}(OH)]^{4+}$ oxide layers parallel to (010) by Sr(1, 5)–O bonds and hydrogen bonds between O(8) and OH ($d_{O(8)-OH}$ = 2.61 Å) (Fig. 3). The layers are slightly wavy. H_2O molecules are located at the wave troughs and complement the coordination sphere of the Sr(5) cations (Fig. 4). There is no hydrogen bonding between water oxygen and other atoms. The space between the oxide layers is occupied by $[SbSe_3]^{3-}$ pyramids and isolated Se^{2-} anions

TABLE 3
Selected Bond Length (Å) and Angles (°) for $Sr_{10}[Sb_7O_{13}(OH)]_2[SbSe_3]_2Se\cdot 2H_2O$

	$[Sb(1–8)O_mSe_n]$ polyhedra				
	Distance	Angles			
Sb1–					
O2	1.968(4)				
O1	1.990(4)	90.2(2)			
OH	2.047(4)	84.5(2)	81.4(2)		
Se4	3.187(1)	76.4(1)	72.9(1)	147.6(1)	
Sb2–					
O10	1.920(4)				
O2	2.000(4)	88.4(2)			
O3	2.021(4)	90.7(2)	84.9(2)		
Se2	3.277(1)	82.9(1)	79.4(1)	163.1(1)	
Se1	3.416(1)	80.9(1)	159.2(1)	77.6(1)	116.47(2)
Sb3–					
O9	1.905(4)				
O3	2.000(4)	89.8(2)			
O4	2.028(4)	89.8(2)	85.7(2)		
Se1	3.374(1)	81.5(1)	78.9(1)	161.8(1)	
Sb4–					
O8	1.948(3)				
O4	1.988(4)	90.2(2)			
O5	2.017(4)	89.5(2)	85.8(2)		
Se2	3.358(1)	75.9(1)	86.0(1)	163.2(1)	
Sb5–					
O7	1.922(4)				
O5	1.981(4)	92.4(2)			
O6	2.091(4)	87.0(2)	85.7(2)		
Se3	3.203(1)	83.3(1)	85.6(1)	166.7(1)	
Sb6–					
O6	1.957(4)				
O1	1.994(4)	90.4(2)			
O11	2.011(4)	90.7(2)	85.5(2)		
Se4	3.182(1)	83.1(1)	73.0(1)	157.5(1)	
Sb7–					
O13	1.914(4)				
O12	1.915(4)	93.6(2)			
O11	2.076(4)	94.3(2)	88.6(2)		
Sb8–					
Se2	2.547(1)				
Se3	2.563(1)	99.58(2)			
Se1	2.564(1)	104.85(2)	100.88(2)		

TABLE 3—*Continued*

Other atoms			
Sr1–		Sr4–	
O12	2.415(4)	O12	2.530(4)
O7	2.457(4)	O1	2.545(4)
OH	2.555(4)	O10	2.564(4)
O2	2.617(4)	O9	2.575(4)
O10	2.650(4)	OH	2.578(4)
Se3	3.304(1)	O3	2.641(4)
Se1	3.318(1)	O11	2.785(4)
Sr2–		Sr5–	
O12	2.542(4)	O13	2.401(4)
O5	2.565(4)	O10	2.452(4)
O13	2.596(4)	O8	2.454(4)
O3	2.607(4)	O7	2.580(4)
O2	2.732(4)	OW	2.689(5)
O6	2.758(4)	O5	2.955(4)
Se4	3.081(1)	Se2	3.478(1)
Sr3–			
O6	2.531(4)		
O9	2.537(4)		
O13	2.565(4)		
O8	2.588(4)		
O7	2.590(4)		
O4	2.741(4)		
Se2	2.311(1)		

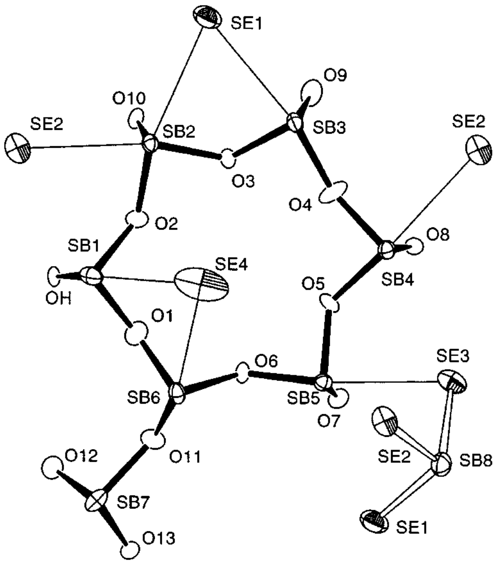

FIG. 1. Coordination environments of the Sb atoms and the single branched six-ring. Weak Sb–Se interactions are drawn with thin lines. Thermal ellipsoids are drawn with 95% probability.

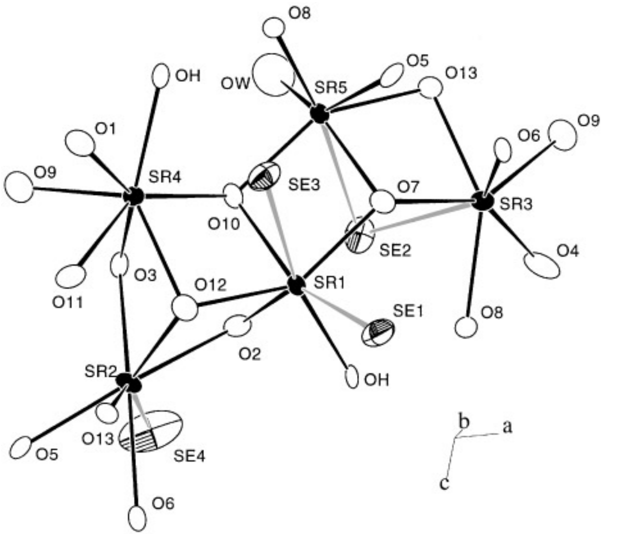

FIG. 2. Coordination environments of the Sr atoms. Thermal ellipsoids are drawn with 95% probability.

(Fig. 4). The oxide layers are held together through ionic Sr–Se bonds and weak interactions between the Sb atoms of the rings and Se atoms. The shortest Sr–Se bonds are those between the Sr(2) cations located near the centers of the six-rings and the interlayer Se(4) anions. However, the thermal ellipsoid of the Se(4) atom is considerably larger than those of the Se(1–3) atoms, suggesting the presence of static disorder probably due to the absence of strong covalent bonds to Se(4) (Fig. 1, 5). Refinements in which the Se(4) position was split between two sites were unstable. The structure can be described as built up from alternating oxide and selenide sheets.

Separation between the oxide and selenide units most likely reflects the substantial size and electronegativity differences between oxygen and slenium. Similar phenomenon can be found in some oxothioantimonates. For example, the structure of the mineral sarabauite $CaSb_{10}O_{10}S_6$ contains $[CaSb_6O_{10}]$ slabs sandwiching $[Sb_4S_6]$ units (10). In the cetineite-type compounds, infinite oxide tubes are surrounded by infinite columns of $[SbS_3]$ or $[SbSe_3]$ pyramids (1, 5).

A far as we can ascertain, the $[Sb_6O_{12}]$ six-rings are found only in the $[Sb_{12}O_{18}]$ tubes of the cetineite-type structure. The tube can be considered as formed from the $[Sb_6O_{12}]$ six-rings in the way that each rings shares its six terminal oxygen atoms with neighboring rings. In fact, the $[Sb_7O_{13}(OH)]$ group found in the title compound can also be considered as a building block for the $[Sb_{12}O_{18}]$ cetineite tubes. As shown in Fig. 6, two $[Sb_7O_{13}(OH)]$ groups can be connected to form a structural unit with three six-rings. Three such units can be connected into a cetineite-type tube. Since the cetineite phase $Sr_6[Sb_{12}O_{18}][SbSe_3]_2(OH)_6$ crystallized together with the title compound, the structural relationship suggests the possibility

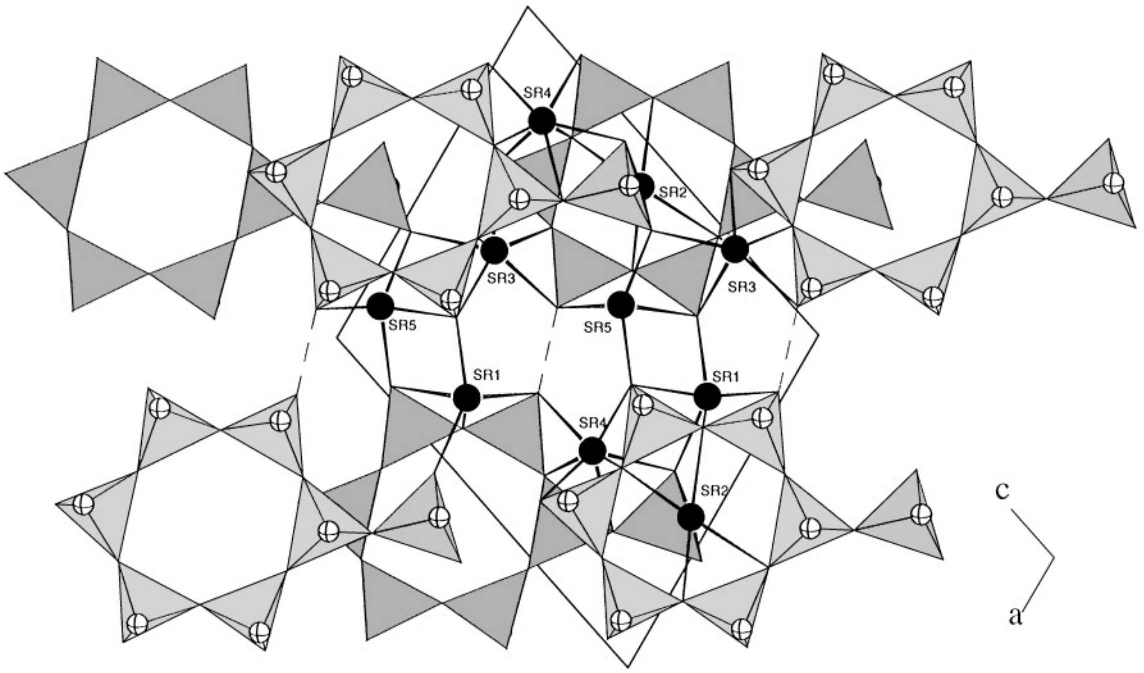

FIG. 3. An oxide layer viewed along [010] showing packing of the rings. Sb atoms are plotted as crossed circles. The hydrogen bonds between the OH and the O(8) atoms are shown by dashed lines.

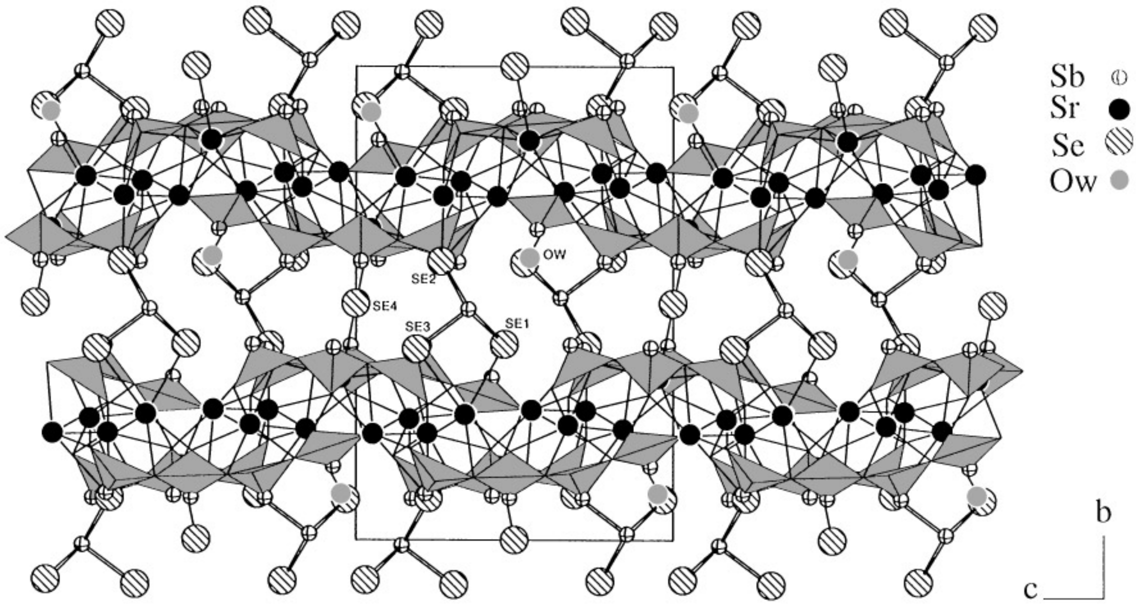

FIG. 4. Projection of the structure along [100].

that $[Sb_7O_{13}(OH)]$ groups might be secondary building units present in solution during the crystallization of both phases. The yield of $Sr_6[Sb_{12}O_{18}][SbSe_3]_2(OH)_6$ can be slightly improved by lowering the $Sr(OH)_2 \cdot 8H_2O$ content of the reactant mixture, but the compound has not yet been synthesized as a single phase.

The bond valence sums calculated with empirical parameters (11) for Sb atoms range from 2.98 to 3.21 v.u. and confirm the trivalent nature of all 8 Sb cations that is indicated by the characteristic pyramidal coordination enviroments. The stereochemically active lone electron pairs (LEP) of the Sb atoms of the oxide layers all point into the interlayer spaces (the selenide sheets). Therefore, the Se^{2-} anions are actually surrounded by the LEP of antimony cations. The structural similarities between the title compound and $K_6[Sb_{12}O_{18}][SbSe_3]_2 \cdot 6H_2O$ suggest that measurements of the photoconductivity of $Sr_{10}[Sb_7O_{13}(OH)]_2[SbSe_3]_2Se \cdot 2H_2O$ would be of interest.

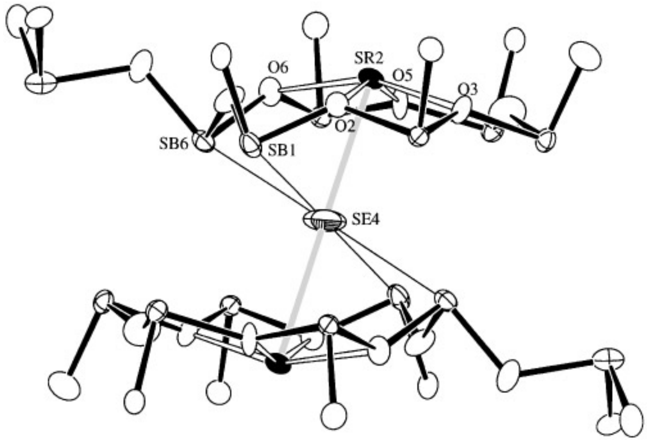

FIG. 5. The coordination environment of the Se(4) anion connecting two six-rings of two neighboring oxide layers through bonds to Sr(2).

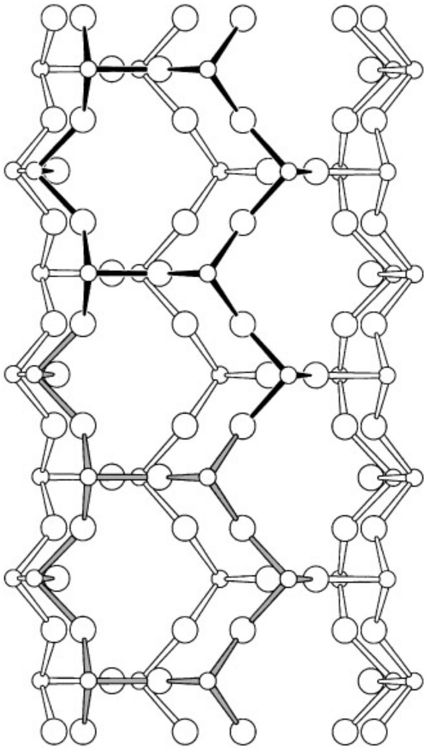

FIG. 6. A cetineite $[Sb_{12}O_{18}]$ tube. Two building blocks corresponding to the single branched six-rings found in the title compound are marked through black and grey solid bonds, respectively.

ACKNOWLEDGMENTS

We appreciate helpful comments by Professor F. Liebau. We thank the National Science Foundation (DMR9214804), the R. A. Welch Foundation for financial support. X. W. thanks the Deutsche Forschungsgemeinschaft for support when he was in the Mineralogisches Institut der Universität Kiel, Germany, where part of the work was performed. This work made use of MRSEC/TCSUH Shared Experimental Facilities supported by the National Science Foundation under Award Number DMR-9632667 and the Texas Center for Superconductivity at the University of Houston.

REFERENCES

1. C. Sabelli, I. Nakai, and S. Katsura, *Am. Mineral.* **73,** 398 (1998).
2. U. Simon, F. Schüth, S. Schunk, X. Wang, and F. Liebau, *Angew. Chem. Int. Ed. Engl.* **36,** 1121 (1997).
3. F. Starrost, E. E. Krasovskii, W. Schattke, J. Jockel, U. Simon, X. Wang, and F. Liebau, *Phys. Rev. Lett.* **80,** 3316 (1998).
4. X. Wang and F. Liebau, *Eur*, *J. Mineral.* **3,** No. 1, 288 (1991).
5. X. Wang and F. Liebau, *Eur. J. Solid State Inorg. Chem.* **35,** 27 (1998).
6. Siemens Analytical X-ray Instruments, SAINT, Version 4.05, Madison, WI, 1995.
7. G. M. Sheldrick, SADABS program, University of Göttingen, 1995.
8. N. Walker and D. Stuart, *Acta Crystallogr. Sect. A* **39,** 158 (1983).
9. G. M. Sheldrick, SHELXTL, Version 5.03, Siemens Analytical X-ray Instruments, Madison, WI, 1995.
10. I. Nakai, K. Nagashima, K. Koto, and N. Morimoto, *Acta Crystallogr. Sect. B* **34,** 3569 (1978).
11. N. E. Brese and M. O'Keefe, *Acta Crystallogr. Sect. B* **47,** 192 (1991).